Bio-Design and Manufacturing (2021) 4:902–911
https://doi.org/10.1007/s42242-021-00140-9

RESEARCH ARTICLE

Fabrication of gelatin methacryloyl hydrogel microneedles for transdermal delivery of metformin in diabetic rats

Zhiyong Zeng[1] · Guohua Jiang[1,2,3] · Tianqi Liu[1] · Gao Song[1] · Yanfang Sun[4] · Xueya Zhang[1] · Yanting Jing[1] · Mingjia Feng[1] · Yufei Shi[1]

Received: 7 January 2021 / Accepted: 1 June 2021 / Published online: 18 June 2021

Abstract

Injection therapy for diabetes has poor patient compliance, and the pain occurring at the site of subcutaneous injections causes significant inconvenience to diabetic patients. In this work, to demonstrate the benefits of an alternative drug delivery technique that overcomes these issues, methacrylated gelatin hydrogel-forming microneedles integrated with metformin were developed to adjust blood glucose levels in diabetic rats. Gelatin methacryloyl microneedles (GelMA-MNs) with different degrees of substitution were successfully prepared by a micro-molding method. The resultant GelMA-MNs exhibited excellent mechanical properties and moisture resistance. Metformin, an anti-diabetic drug, was further encapsulated into the GelMA-MNs, and its release rate could be controlled by the three-dimensional cross-linked network of microneedles, thereby exhibiting sustained drug release behaviors in vitro and implying a better therapeutic effect compared with that of subcutaneous injection in diabetic rats. The drug release period could be significantly prolonged by improving the cross-link density of GelMA-MNs. The results of hypoglycemic effect evaluation show that the application of GelMA-MNs for transdermal delivery in diabetic rats has promising benefits for diabetes treatment.

✉ Guohua Jiang
ghjiang_cn@zstu.edu.cn

✉ Yanfang Sun
katherineyfs@zstu.edu.cn

[1] School of Materials Science and Engineering, Zhejiang Sci-Tech University, Hangzhou 310018, China

[2] Institute of Smart Biomedical Materials, Zhejiang Sci-Tech University, Hangzhou 310018, China

[3] Zhejiang-Mauritius Joint Research Center for Biomaterials and Tissue Engineering, Zhejiang Sci-Tech University, Hangzhou 310018, China

[4] College of Life Sciences and Medicine, Zhejiang Sci-Tech University, Hangzhou 310018, China

Graphic abstract

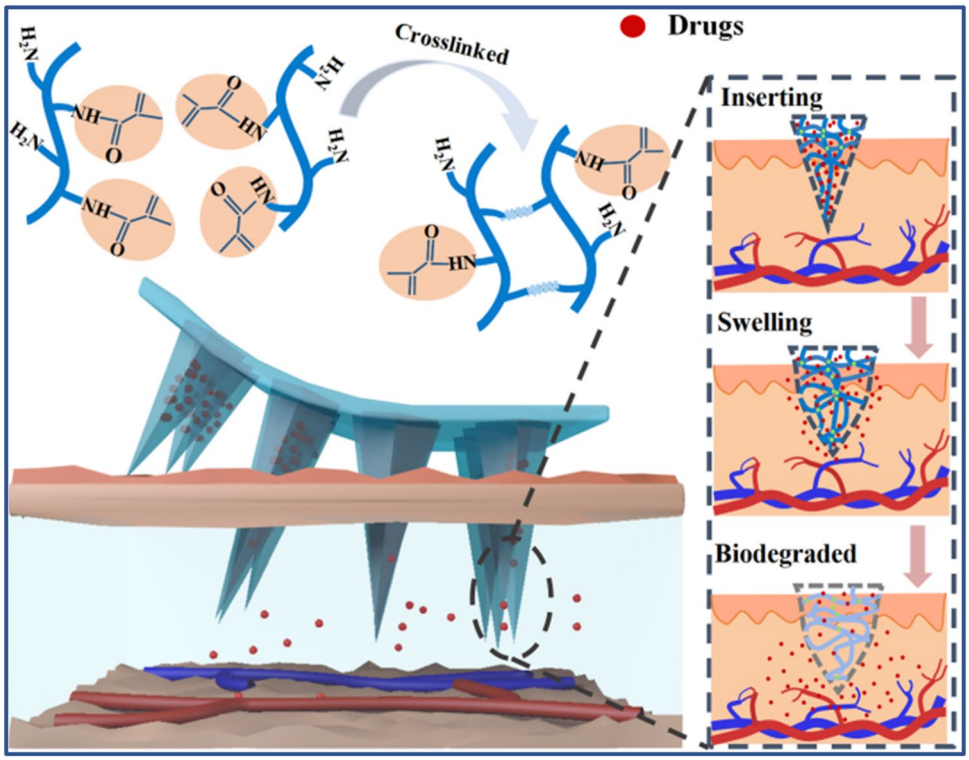

Keywords Microneedles · Metformin · Transdermal delivery · Biodegradable · Gelatin · Hypoglycemic effect

Introduction

Diabetes mellitus, characterized by a high level of blood glucose, is a kind of chronic disease when the pancreas is unable to make insulin or the cells cannot well respond to the insulin produced and is identified as a significant health problem in the world [1]. According to the latest report from the International Diabetes Federation (IDF), an estimated 463 million people suffered with diabetes in 2019 and this number was predicted to rise to 700 million by 2045 [2]. At present, the subcutaneous injection of insulin is a common method to treat diabetic patients. Nevertheless, the frequent injection of insulin leads to needle phobia and poor patient compliance, and also increases the risk of infections [3, 4]. Hypoglycemia, a threatening condition for patient life, may even occur after the administration with insulin over the required dose [5]. Therefore, minimally invasive and more convenient routes have been widely studied to overcome these disadvantages. However, traditional noninvasive drug delivery routes, such as oral or transdermal, have shown limited utility value.

Transdermal drug delivery methods would provide an attractive alternative for the delivery of injectable drugs owing to their better patient compliance, ease of self-administration, avoidance of first-pass metabolism, as well as the circumvention of gastric degradation. The skin is a natural physical barrier protecting the body from diseases by the stratum corneum (SC), which is the greatest challenge for transdermal drug administration. The outer layer of SC limits drug diffusion through the skin, and only a limited drug dose can be delivered through this route [6]. Numerous approaches to enhance drug permeability have been proposed to overcome this limitation. Among them, the technology of microneedles (MNs) as a novel transdermal drug delivery system has emerged with a promising potential to improve the efficacy of transdermal drug delivery [7, 8]. The concept of MNs was first reported in 1970, which combines the merits of subcutaneous injection and traditional transdermal drug delivery [9]. The MNs are micron-sized needles that are long enough to pierce the SC, but too short to irritate the pain receptors located in the dermis [10, 11]. Many materials have been utilized to manufacture MNs, including metal, glass, silicon, polymer, ceramics, and others. However, safety issues persist due to their lower biocompatibility and limited drug loading capacity [12, 13]. Among them, polymers are considered as ideal materials for manufacturing MNs because of their favorable processability,

good biocompatibility and tailorable functionality. Various polymer materials, including hyaluronic acid [14], silk fibroin [15], chitosan [16], and polyvinyl acetate [17], have been used to fabricate MNs. To date, less attention has been paid to sustained drug release by microneedles in diabetes research, which would be beneficial for avoiding a hypoglycemic effect caused by burst release.

Hydrogels have a three-dimensional network that can absorb liquid by swelling and maintain their structural integrity. They are widely applied in biomedical fields, including tissue engineering and drug delivery, because of their porous structure and excellent biocompatibility [18, 19]. However, the weaker mechanical properties of hydrogels prepared from natural materials hinders their wider application [20]. Compared with natural polymers, synthetic polymer materials have excellent mechanical performance but lower biocompatibility and biodegradation rate. Therefore, it is preferable to combine the merits of natural and synthetic polymer materials. Gelatin with good biocompatibility and biodegradability is derived from collagen and can be inexpensively obtained in a range of forms while maintaining cell binding sequences, such as matrix metal loproteinase (MMP)-sensitive biodegradation sites [21]. However, the mechanical properties of pure gelatin microneedles are insufficient for puncturing the stratum corneum. Tunable mechanical properties of gelatin hydrogels can be obtained by adjusting the structure and type of substituents. For example, gelatin-methacrylamide is a gelatin derivative that can be obtained by modifying the amine groups of gelatin with methacrylate groups [22, 23]. GelMA prepared by the grafting of methacrylic anhydride onto gelatin exhibits excellent photocurability and can be cross-linked by exposure to ultraviolet (UV) in the existences of photoinitiators. This enables GelMA microneedles to have sufficient mechanical toughness to pierce the skin, making it an attractive material for microneedle technology [24, 25].

Herein, we characterized GelMA as an inexpensive, cell-responsive hydrogel platform for creating microneedle devices. The morphology, mechanical behaviors, and swelling abilities of GelMA microneedles (GelMA-MNs) were assessed, and the skin insertion and drug release profiles of MNs were evaluated in vitro. The obtained MNs were used to demonstrate the transdermal delivery of metformin. The hypoglycemic effect of metformin-loaded microneedles was investigated in a diabetic rat model.

Materials and methods

Chemicals

Gelatin (medicinal grade, type B), methacrylic anhydride (MA), rhodamine 6G (R6G), phosphate buffer solution (PBS) and 2-hydroxy-4'-(2-hydroxyethoxy)-2-methylpropiophenone (Irgacure 2959) were obtained from Shanghai Aladdin Bio-Chem Technology Co., Ltd. (Shanghai, China). Normal saline (NS), metformin hydrochloride (Met), streptozotocin (STZ) and agar were purchased from Sigma-Aldrich. Male Sprague–Dawley (SD) rats were provided by Zhejiang Academy of Medical Science, Hangzhou, China. All the chemical reagents were used without further purification except ultrapure water, which was produced in a water purification system. The GelMA was prepared according to previous reports [26–28].

Fabrication of GelMA-MNs

Microneedle patches were fabricated by the previously described method [29, 30]. Briefly, 0.6 g GelMA prepolymer was added into 2 mL of deionized water at 45 °C. Next, 10 mg of photoinitiator (Irgacure 2959) and 300 mg of metformin hydrochloride were dissolved in the above solution. A volume of 200 μL of the blended solution was casted onto the surface of polydimethylsiloxane (PDMS) molds according to the previous reports [31, 32]. The molds were subsequently exposed to 10 mW/cm^2 UV light (365 nm) for 5 min, followed by drying for 12 h. Finally, the GelMA-MNs were gently peeled off from PDMS molds and stored before use.

Mechanical and skin penetration tests in vitro

The mechanical performance of GelMA-MNs was assessed by a universal material testing machine (WDW-02, Tianchen Testing Machine Co. LTD., Jinan, China). The microneedle patch was horizontally fixed to an aluminum base plate. The movement speed of the top stainless plate was 0.3 mm/s. The force–displacement curve was recorded by the testing system when the top stainless plate came into contact with the microneedles. For the skin penetration test, GelMA-MNs loaded with R6G were perforated into stretched rat skin tissues compressed by an index finger continuously for 5 min, then the backing patches were gently separated. The skin was embedded and frozen in an O.C.T. compound, and then cut into 7 μm sections used for histological observation by a confocal laser scanning microscope (CLSM, C2, Nikon Corporation, Japan).

Swelling ability of GelMA-MNs

For the evaluation of swelling ability, GelMA-MNs with different degrees of crosslinking were immersed in DPBS or inserted into a 2.0 wt% agarose hydrogel for 1, 3, 7, 15, and 20 min at 37 °C [33]. The initial weight (W_i) of each GelMA-MNs sample was measured by a precision electronic balance (JF2004, Yuyao Jinnuo Balance Instrument Co., Ltd., China) before insertion into agarose hydrogel. At

each predetermined time point, the mass (W_f) of GelMA-MNs was recorded after the removal of surface residual water by tissue paper. The swelling ratio was defined via the equation of $[(W_f - W_i)/W_i] \times 100\%$.

Drug encapsulation and drug release in vitro

GelMA-MNs with different degrees of crosslinking were loaded with metformin to determine their drug encapsulation ability and drug release kinetics. The standard curve of metformin was analyzed firstly by an UV–vis absorption spectrophotometer (TU-1901, Beijing Purkinje General Instrument Co., Ltd., China) at a wavelength of 233 nm [34, 35]. The as-fabricated microneedles were randomly selected and immersed in deionized water until completely dissolved, and the absorbance of the uniform solution was measured by UV–vis. The drug release kinetics in vitro were tested by embedding metformin-loaded microneedles into agarose hydrogel, and then removing the patches. At each time point, the absorbance of metformin released from microneedles was obtained by measuring the metformin concentration in the residual patches. The metformin loading capacity and release behavior were quantified by dividing the residual metformin in the backing of patches and calculated according to the standard curve for metformin.

Hypoglycemia effect on diabetic rats in vivo

The diabetic rat model was firstly established by injecting STZ (10 mg/mL in normal saline) into SD rats (200 ± 20 g). All animals were fed with food and water ad libitum to acclimate for 2 weeks before the experiment. Blood samples were collected from the vein of rats to measure their blood glucose levels via a glucometer (Sinocare Inc., Changsha, China). After the plasma glucose levels reached the stable hyperglycemia status, the diabetic rats were randomly divided into five groups ($n = 3$ for each group): (1) control groups without any treatment; (2) subcutaneous injection groups (10 mg/kg); (3) microneedle groups treated by GelMA1-MNs, GelMA2-MNs and GelMA3-MNs. In order to evaluate the hypoglycemic effect using the as-prepared GelMA-MNs as a transdermal delivery platform, rat blood glucose levels were monitored over time after feeding (2 g). In addition, to further assess the pharmacokinetics and long-term hypoglycemia effect of microneedle patches, six diabetic rats were randomly selected and divided into two groups following three daily meals (breakfast, lunch, and dinner). At each desired time point, the blood glucose level of each rat was measured until the return to the initial level of hyperglycemia.

Acute toxicity assay

In order to evaluate acute toxicity in vivo, SDs treated with MNs were selected randomly as the experimental group, and SDs without treatment were used as the control group [36, 37]. The major organs, including the heart, liver, spleen, lung and kidney of the rats, were collected for acute toxicity assay. Histological examinations were characterized by a fluorescence inversion microscope.

Results and discussions

Preparation of GelMA microneedles

In this work, the GelMAs with different graft degrees were firstly synthesized by controlling the molar ratio of MA and gelatin separately at 6:1, 11:1 and 17:1 [38], and the obtained GelMAs were denoted as GelMA1, GelMA2, and GelMA3, respectively. The successful preparation of GelMAs with different degrees of methacrylation was confirmed by Fourier-transform infrared spectrometer (FTIR) and ^{1}H NMR analysis, as shown in Fig. S1. The absorption band at 1649 cm^{-1} is attributed to C = O stretching vibration (amide I). The absorption peaks at 1547 cm^{-1} and 1241 cm^{-1} are ascribed to N–H bending coupled to C–N stretching (amide II), and N–H bending and C–N stretching (amide III), respectively. A typical absorption peak appears around 3360 cm^{-1} owing to the N–H stretching vibration [39]. In comparison to pure Gel, new peaks at 5.6, 5.3 and 1.8 ppm can be observed, which are associated with proton signals from the acrylic and methyl group, respectively (Fig. S2) [40]. The graft degree is defined as the integral area ratio of methacrylate groups to the unmodified amino group of gelatin [41]. The graft degrees were 62.8%, 71.3%, and 92.3% obtained for GelMA1, GelMA2, and GelMA3, respectively (Table S1).

The hydrogel microneedles were prepared by casting prepolymer with or without metformin into polydimethylsiloxane (PDMS) microneedle mold, and then cross-linked by UV irradiation. As shown in Fig. 1a, the hydrogel microneedles consisted of 10×10 needles distributed on a 1 cm^2 supporting layer by using a micro-molding process (Fig. 1b). The as-prepared MNs present pyramidal needle morphology (Fig. 1c). The total height of MNs and the tip-to-tip distance of adjacent MNs is about 600 μm and 500 μm, respectively. The supporting substrate of MNs has a base width of about 200 μm (Fig. 1d–1f).

Mechanical and skin insertion tests of GelMA-MNs

The mechanical properties of MNs are a critical factor to achieve their successful insertion into the skin [42,

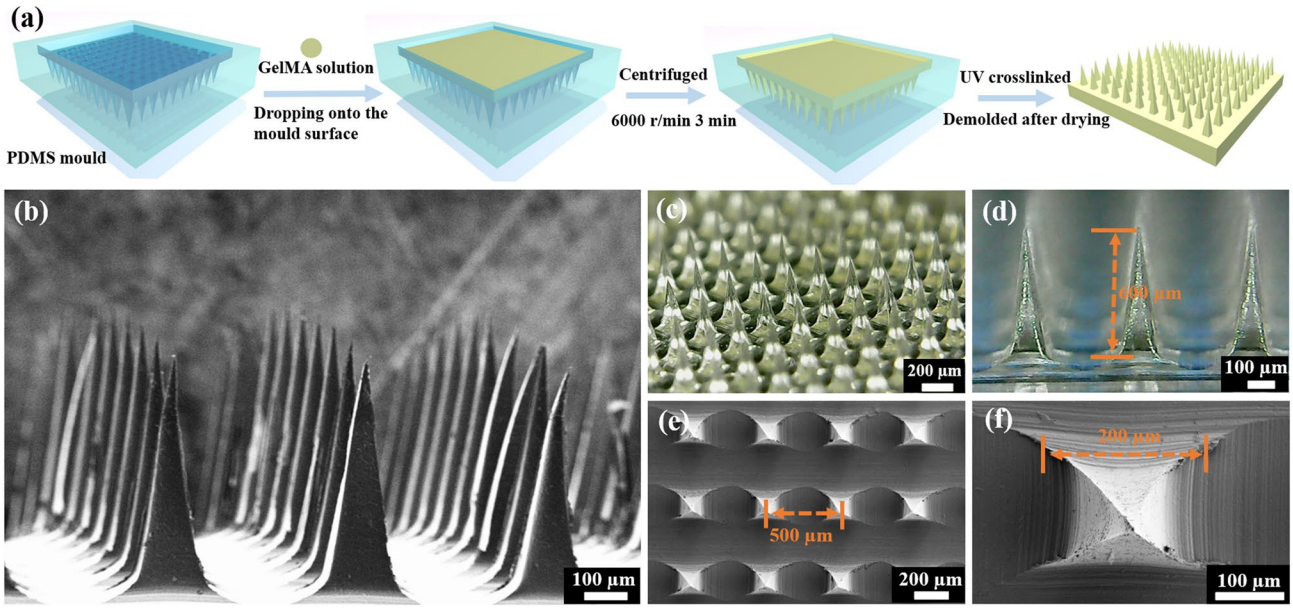

Fig. 1 Preparation and characterization of GelMA-MNs. **a** Schematic illustration of GelMA-MNs fabrication process. **b** SEM image of microneedle (side view). **c, d** Bright-field microscopy image of MNs. **e, f** SEM images of MNs (top view) and corresponding high magnification area of a single needle

43]. The mechanical performance of hydrogel MNs was investigated by a compression test. As shown in Fig. 2a, neither discontinuity can be found in the force–displacement curves, nor fracture and broken MNs can be observed at 600 μm displacement (Fig. 2b), implying the excellent toughness of GelMA-MNs. The maximum force measured at 600 μm displacement was 0.9, 1.2, 1.9 N needle^{-1} for GelMA1-MNs, GelMA2-MNs, and GelMA3-MNs, respectively, which all satisfy the demand value of approximately 0.1 N needle^{-1} reported for skin piercing via MNs [44, 45]. To investigate whether the prepared MNs enable complete skin penetration, GelMA-MNs were inserted into rat cadaver skin using an in-house made applicator. Firstly, rhodamine 6G (R6G), a red fluorescent dye for visualization, was loaded into MNs. As shown in Fig. 2c, the MNs patch can be successfully embedded in the skin and separated from the supporting substrate after penetration for 5 min with an application force of approximately 10 N per needle. The skin surface was left with a complete array of red puncture dots, implying that all needles had penetrated into the skin. Histological sections clearly demonstrated that the MNs could completely penetrate into the skin at approximately 500 μm depth (Fig. 2d). Drug-embedded MNs can be diffused in skin tissue with the assistance of the skin interstitial fluid, as shown in the bright-field images (Fig. 2e).

Swelling property and ex vivo drug release profile of GelMA-MNs

The swelling property of hydrogel MNs is an important parameter for sustained drug release in vivo [46–48]. In order to evaluate their swelling ability, GelMA-MNs prepared from different degrees of methacrylated gelatin were embedded into PBS solution. The hydrogel MNs absorbed moisture quickly, which resulted in the volume expansion of microneedle arrays. Although the swelling ratio of the three GelMA-MNs arrived at an equilibrium within 5 min where the hydrogel network reached a saturation state, the swelling speeds were remarkably different between the three MNs made by different methacrylated gelatin prepolymer (Fig. S3). In order to simulate the penetration of MNs into the skin, GelMA-MNs were further embedded into agarose hydrogel, and their weight gain was monitored over time [49]. As shown in Fig. 3a, the swelling ratio was improved with increased insertion time. A lower grafting degree resulted in a higher swelling ratio due to the absorption of moisture from the agarose hydrogel. The MNs still kept their original morphology after removal from the agarose hydrogel, indicating that they cannot be dissolved immediately in skin tissue. After the loading of R6G, the observed swelling properties were more obvious. The half-height width was about 100 μm for the swelled MNs, which consisted

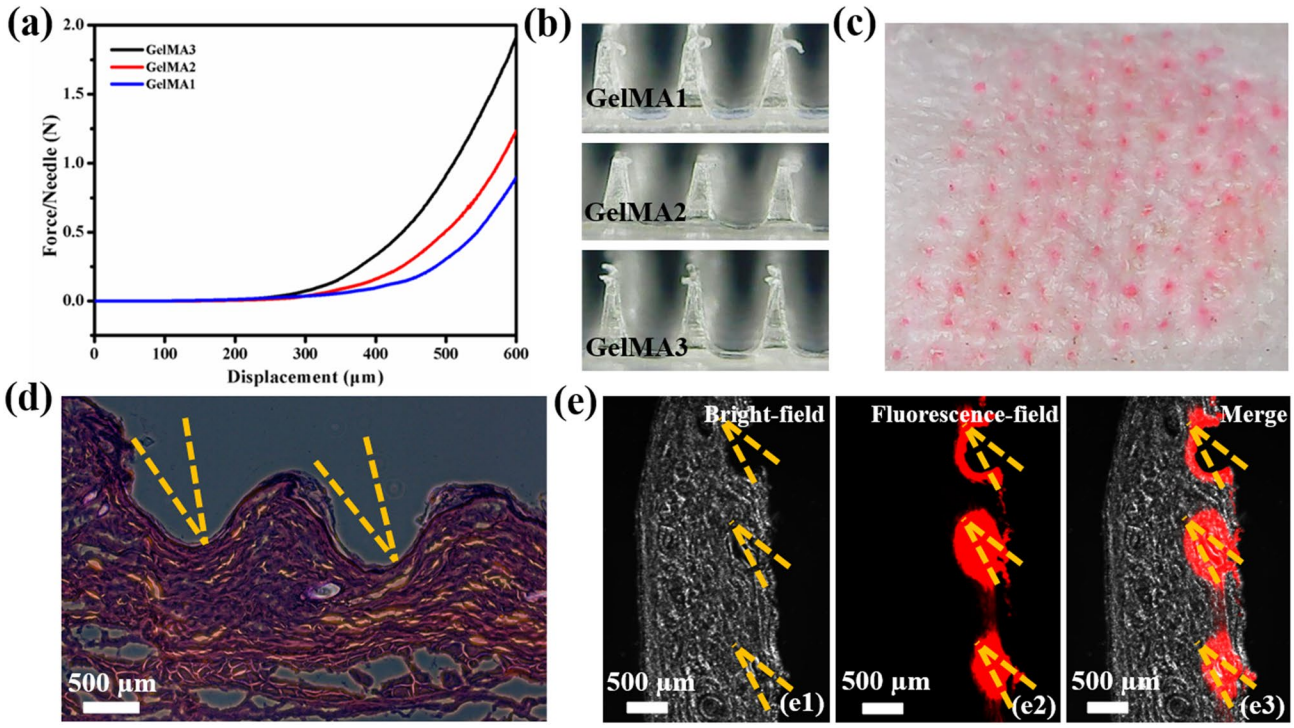

Fig. 2 Mechanical behavior of GelMA-MNs. **a** Force–displacement curve of GelMA-MNs with different crosslinking densities. **b** Optical images of MNs after compression at 400 μm. **c** Rat skin treated with MNs loaded with R6G (bright-field image). **d** H&E-stained histological section image characterized by optical microscope. **e** Fluorescent images of histological section characterized by CLSM

an increase compared with about 80 μm for the unswelled ones (Fig. 3b).

Metformin is one of the most widely prescribed drugs for the treatment of type 2 diabetes mellitus patients [50–52]. Herein, metformin release profile in vitro was investigated to assess the sustained drug release properties of MNs (Fig. S4). Figure 3c reveals the release behaviors of metformin released from the MNs embedded in agarose hydrogel. The drug loaded in the three kinds of GelMA-MNs was released continuously and reached 80.6%, 72.7% and 65.2% of the total loading volume in 11 min, respectively. Metformin release occurred in a continuous pattern, and no burst release could be observed in the first few minutes. In addition, lower metformin release could be obtained from the MNs with higher grafting degree due to correspondingly higher crosslinking density after polymerization. These results indicate that the quantity of released drug molecules was proportional to the swelling rate of the MNs polymer network. CLSM was used to reconstruct the morphology of MNs in rat skin tissue. As demonstrated in Fig. 3d, the MNs exhibit a pyramidal morphology prior to insertion into skin. After skin penetration, the MNs still can keep their original morphology, however, MNs gradually dissolve with the prolongation of penetration time. These findings demonstrate that the swelling property of GelMA-MNs provides allow the realization of sustained drug delivery in vivo.

Hypoglycemic effect in vivo

In order to investigate their pharmacological effect, metformin-loaded MNs were administered to type 2 diabetic rats induced by STZ [53, 54]. The healthy group and the blank group (without any treatment) were used as negative control, and the diabetic rats treated with a hypodermic injection of metformin (2 mg) were chosen as positive control. To evaluate the hypoglycemic effect of MNs, the blood glucose levels (BGLs) of treated rats in each group were monitored over time. As shown in Fig. 4a, the BGL of diabetic SD rats increased to about 600 ± 40 mg/dL within 1 h after feeding with fodder. Following the subcutaneous injection, the BGL reached the lowest level (139 ± 20 mg/dL) at 2 h, and then returned quickly to its original state, thus showing an obvious short-term hypoglycemic effect. In the MNs groups, a steady decline of BGL was observed. The lowest BGL could be observed after administration at 2.5, 3.5 and 4 h. The higher cross-link density of MNs causes a longer hypoglycemic effect. Figure 4b depicts the changes of BGLs for unfed rats. The BGLs for the group with higher cross-link density of MNs can be maintained for a longer period. To further investigate the effect of feeding on the BGL, diabetics rats were treated thrice daily with standardized meals. The BGLs exhibited a curve that fluctuates with feeding, as shown in Fig. 4c. In the MNs group, however, the BGLs reached the highest value 2 h after the first feeding and

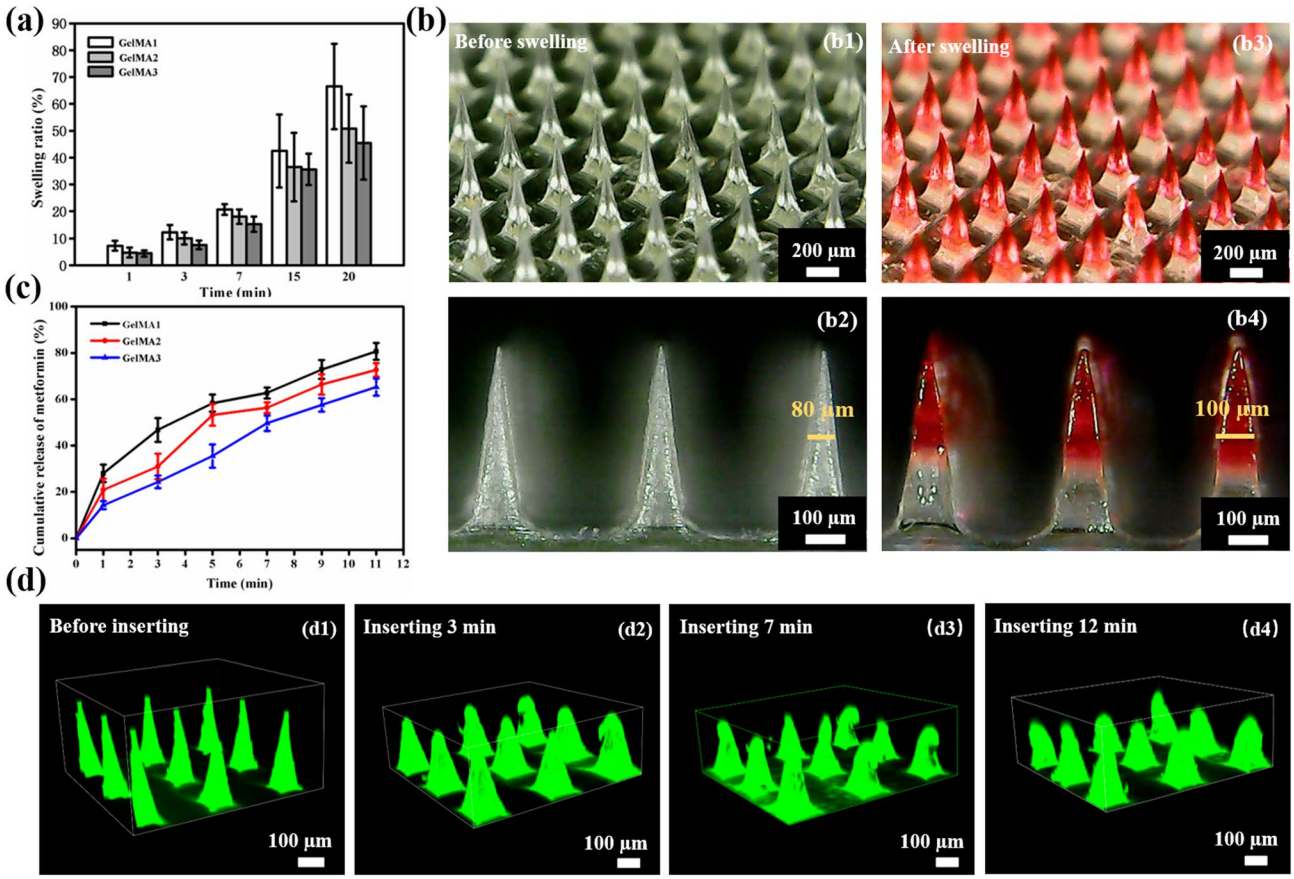

Fig. 3 Swelling property of MNs. **a** Swelling ratio of GelMA1, GelMA2 and GeMA3 in agarose hydrogel ($n=5$ for each group). **b** Optical microscope images of GelMA3 swelling taken 3 min after removal from agarose hydrogel. **c** Drug release profile in agarose hydrogel ($n=5$ for each group). **d** Swelling behavior of GelMA1 MN in rat skin tissue

decreased to the lowest value of about 200 mg/dL 4 h after the first feeding. In the second and third feeding cycles, similar BGL curves could also be observed, showing an initial and sustained drug delivery behavior response to BGLs, as well as better hypoglycemic effect, when compared with hypodermic administration.

In addition, to evaluate whether the administration of MNs result in tissue damage in the body, H&E staining images of the main organs, including the heart, liver, spleen, lung and kidney, were carried out [55]. As shown in Fig. 4d, no significant changes occurred in tissue morphology in the MNs group compared with the control group, which indicates the hypotoxic characteristic of as-fabricated MNs and, as the tissue lesion caused was negligible, their promising value for clinical applications.

Conclusions

In this paper, hydrogel MNs fabricated from methacrylated gelatin were developed. The as-prepared microneedles exhibited pyramidal morphology and showed sufficient mechanical properties to puncture the rat skin. The swelling behavior and mechanical strength of the obtained MNs could be controlled by adjusting the crosslinking density. The higher grafting degree of methacrylated gelatin exhibited higher mechanical strength, lower swelling ratios, and slower metformin release behaviors. The structural integrity of proposed GelMA-MNs can be maintained in the simulated skin tissue and allows the release of encapsulated metformin in a satisfactory initial and sustained dose.

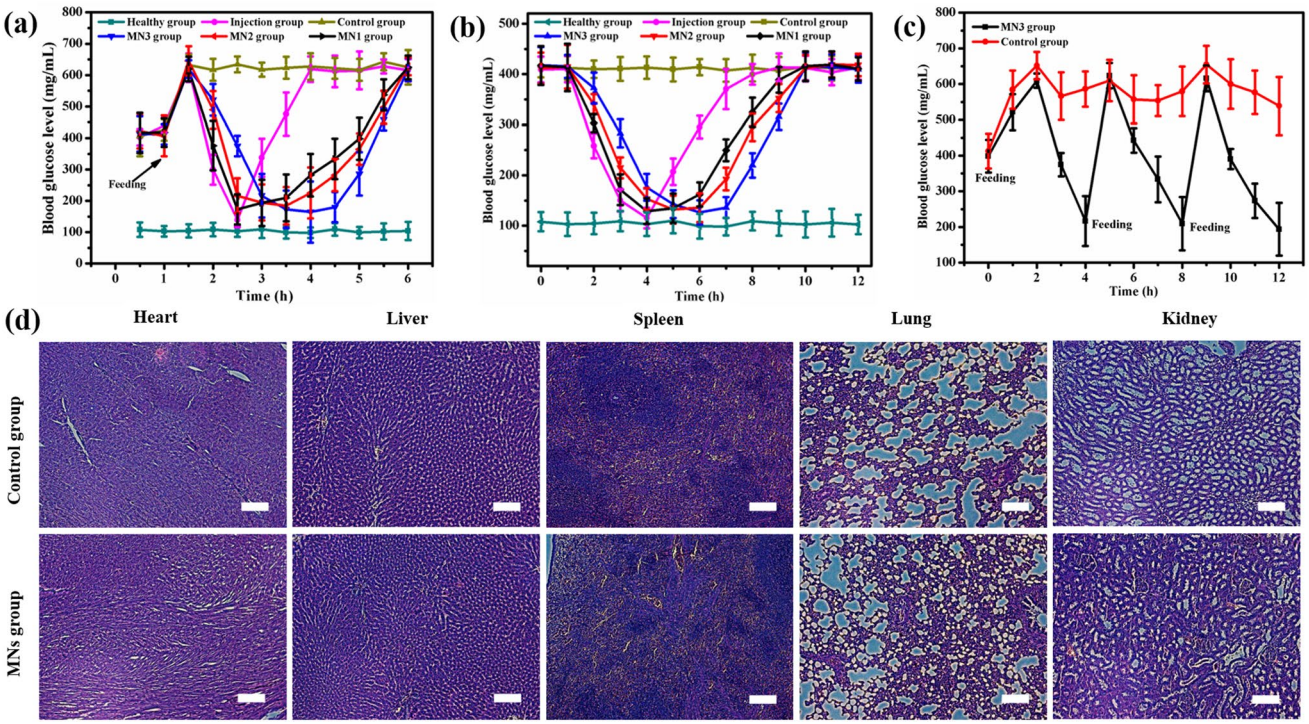

Fig. 4 Hypoglycemic effect. **a, b** Blood glucose level of rats treated with metformin-loaded MNs with different degree of crosslinking, fed once and unfed, respectively ($n=3$ for each group). **c** Blood glucose level of rats in 12 h post-treatment, fed three times ($n=3$ for each group). **d** H&E staining images of tissues from the main organs, such as the heart, liver, spleen, lung and kidney, characterized by an optical microscope. Scale bar, 100 μm

The hypoglycemic effect was investigated on the diabetic rats induced by STZ in vivo and compared with hypodermic injections. The obtained metformin-loaded MNs exhibited a promising hypoglycemic effect, hypotoxicity, and weak inflammation stimulation reaction, thereby indicating their potential clinical application value.

Supplementary Information The online version contains supplementary material available at https://doi.org/10.1007/s42242-021-00140-9.

Acknowledgements This work was supported by the National Natural Science Foundation of China (No. 51873194) and the Natural Science Foundation of Zhejiang Province, China (No. LY18E030006). We also gratefully acknowledge Zhejiang Academy of Medical Science for histological experiments.

Author contributions ZYZ and GHJ contributed to conceptualization; ZYZ contributed to the experimental research; GHJ and YF Sun contributed to resources, funding acquisition and supervision; XYZ, GS, and TQL contributed to methodology; ZYZ contributed to writing; YTJ, MJF, and YF Shi helped in animal experimental research and data analysis; GHJ reviewed and edited the manuscript.

Declarations

Conflict of interest The authors declare that there is no conflict of interest.

Ethical approval All institutional and national guidelines for the care and use of laboratory animals were followed. All the animal procedures were reviewed and approved by the Animal Ethics Committee of Zhejiang Sci-Tech University (acceptance number: 2019-02-01).

References

1. Tabák AG, Herder C, Rathmann W et al (2012) Prediabetes: a high-risk state for diabetes development. Lancet 379(9833):2279–2290. https://doi.org/10.1016/S0140-6736(12)60283-9
2. International Diabetes Federation (2019) IDF Diabetes Atlas 9th Edition Brussels: IDF; www.idf.org/diabetesatlas.
3. Chen G, Yu J, Gu Z (2019) Glucose-responsive microneedle latches for diabetes treatment. J Diabetes Sci Technol 13(1):41–48. https://doi.org/10.1177/1932296818778607
4. Yu JC, Zhang YQ, Sun WJ et al (2017) Insulin-responsive glucagon delivery for prevention of hypoglycemia. Small 13(19):1603028. https://doi.org/10.1002/smll.201603028
5. Casparie AF, Elvino LD (1985) Severe hypoglycemia in diabetic patients: frequency, causes, prevention. Diabetes Care 8(2):141–145. https://doi.org/10.2337/diacare.8.2.141
6. Gao Y, Hou MM, Yang RH et al (2019) Highly porous silk fibroin scaffold packed in PEGDA/sucrose microneedles for controllable transdermal drug delivery. Biomacromol 20(3):1334–1345. https://doi.org/10.1021/acs.biomac.8b01715
7. Sharma S, Hatware K, Bhadane P et al (2019) Recent advances in microneedle composites for biomedical applications: advanced

drug delivery technologies. Mater Sci Eng C 103:109717. https://doi.org/10.1016/j.msec.2019.05.002
8. Hao Y, Chen YW, He XL et al (2020) Near-infrared responsive 5-fluorouracil and indocyanine green loaded MPEG-PCL nanoparticle integrated with dissolvable microneedle for skin cancer therapy. Bioact Mater 5(3):542–552. https://doi.org/10.1016/j.bioactmat.2020.04.002
9. Larraneta E, Lutton REM, Woolfson AD et al (2016) Microneedle arrays as transdermal and intradermal drug delivery systems: materials science, manufacture and commercial development. Mater Sci Eng R 104:1–32. https://doi.org/10.1016/j.mser.2016.03.001
10. Prausnitz MR (2004) Microneedles for transdermal drug delivery. Adv Drug Delivery Rev 56(5):581–587. https://doi.org/10.1016/j.addr.2003.10.023
11. Jamaledin R, Yiu CKY, Zare EN et al (2020) Advances in antimicrobial microneedle patches for combating infections. Adv Mater 32(33):2002129. https://doi.org/10.1002/adma.202002129
12. Singh P, Carrier A, Chen YL et al (2019) Polymeric microneedles for controlled transdermal drug delivery. J Contr Release 315(10):97–113. https://doi.org/10.1016/j.jconrel.2019.10.022
13. Kim S, Yang H, Eum J et al (2020) Implantable powder-carrying microneedles for transdermal delivery of high-dose insulin with enhanced activity. Biomaterials 232:119733. https://doi.org/10.1016/j.biomaterials.2019.119733
14. Zheng MJ, Wang ZF, Chang H et al (2020) Osmosis-powered hydrogel microneedles for microliters of skin interstitial fluid extraction within minutes. Adv Healthcare Mater 9(10):1901683. https://doi.org/10.1002/adhm.201901683
15. Tsioris k, Raja WK, Pritchard EM, et al (2012) Fabrication of silk microneedle for controlled-release drug delivery. Adv Funct Mater 22(2):330–335. https://doi.org/10.1002/adfm.201102012
16. Chi JJ, Zhang XX, Chen CW et al (2020) Antibacterial and angiogenic chitosan microneedle array patch for promoting wound healing. Bioact Mater 5(2):253–259. https://doi.org/10.1016/j.bioactmat.2020.02.004
17. Zhang YQ, Wang JQ, Yu JC et al (2018) Bioresponsive microneedles with a sheath structure for H_2O_2 and pH cascade-triggered insulin delivery. Small 14(14):1704181. https://doi.org/10.1002/smll.201704181
18. Kim M, Jung B, Park JH (2012) Hydrogel swelling as a trigger to release biodegradable polymer microneedles. Biomaterials 33(2):668–678. https://doi.org/10.1016/j.biomaterials.2011.09.074
19. Ying GY, Jiang N, Yu CJ et al (2018) Three-dimensional bioprinting of gelatin methacryloyl (GelMA). Bio-Des Manuf 1(4):215–224. https://doi.org/10.1007/s42242-018-0028-8
20. Kong B, Chen Y, Liu R et al (2020) Fiber reinforced GelMA hydrogel to induce the regeneration of corneal stroma. Nat Commun 11(1):1435. https://doi.org/10.1038/s41467-020-14887-9
21. Nichol JW, Koshy ST, Bae H et al (2010) Cell-laden microengineered gelatin methacrylate hydrogels. Biomaterials 31(21):5536–5544. https://doi.org/10.1016/j.biomaterials.2010.03.064
22. Chen YC, Lin RZ, Qi H et al (2012) Functional human vascular network generated in photocrosslinkable gelatin methacrylate hydrogels. Adv Funct Mater 22(10):2027–2039. https://doi.org/10.1002/adfm.201101662
23. Ying GL, Jiang N, Parra-Cantu C et al (2020) Bioprinted injectable hierarchically porous gelatin methacryloyl hydrogel constructus with shape-memory properties. Adv Funct Mater 30(46):2003740. https://doi.org/10.1002/adfm.202003740
24. Yue K, Li XY, Schrobback K et al (2017) Structural analysis of photocrosslinkable methacryloyl-modified protein derivatives. Biomaterials 139:163–171. https://doi.org/10.1016/j.biomaterials.2017.04.050
25. Lee K, Xue YM, Lee J et al (2020) A patch of detachable hybrid microneedle depot for localized delivery of mesenchymal stem cells in regeneration therapy. Adv Funct Mater 30(23):2000086. https://doi.org/10.1002/adfm.202000086
26. Fares MM, Sani ES, Lara RP et al (2018) Interpenetrating network gelatin methacryloyl (GelMA) and pectin-g-PCL hydrogels with tunable properties for tissue engineering. Biomater Sci 6(11):2938–2950. https://doi.org/10.1039/C8BM00474A
27. Noshadi I, Hong S, Sullivan KE et al (2017) *In vitro* and *in vivo* analysis of visible light crosslinkable gelatin methacryloyl (GelMA) hydrogels. Biomater Sci 5(10):2093–2105. https://doi.org/10.1039/C7BM00110J
28. Luo ZM, Sun WJ, Fang J et al (2019) Biodegradable gelatin methacryloyl microneedles for transdermal drug delivery. Adv Healthcare Mater 8(3):1801054. https://doi.org/10.1002/adhm.201801054
29. Zhu JX, Zhou XW, Kim HJ et al (2020) Gelatin methacryloyl microneedle patches for minimally invasive extraction of skin interstitial fluid. Small 16(16):1905910. https://doi.org/10.1002/smll.201905910
30. Yu WJ, Jiang GH, Liu DP et al (2017) Fabrication of biodegradable composite microneedles based on calcium sulfate and gelatin for transdermal delivery of insulin. Mater Sci Eng C 71(1):725–734. https://doi.org/10.1016/j.msec.2016.10.063
31. Chen MC, Huang SF, Lai KY et al (2013) Fully embeddable chitosan microneedles as a sustained release depot for intradermal vaccination. Biomaterials 34(12):3077–3086. https://doi.org/10.1016/j.biomaterials.2012.12.041
32. Yu WJ, Jiang GH, Liu DP et al (2017) Transdermal delivery of insulin with bioceramic composite microneedles fabricated by gelatin and hydroxyapatite. Mater Sci Eng C 73(1):425–428. https://doi.org/10.1016/j.msec.2016.12.111
33. He RY, Niu Y, Li ZD et al (2020) A hydrogel microneedle patch for point-of-care testing based on skin interstitial fluid. Adv Healthcare Mater 9(4):1901201. https://doi.org/10.1002/adhm.201901201
34. Migdadi EM, Courtenay AJ, Tekko IA et al (2018) Hydrogel-forming microneedles enhance transdermal delivery of metformin hydrochloride. J Contr Release 285:142–151. https://doi.org/10.1016/j.jconrel.2018.07.009
35. Zhang Y, Jiang GH, Yu WJ et al (2018) Polymer microneedles fabricated from alginate and maltose for transdermal delivery of insulin. Mater Sci Eng C 85(1):18–26. https://doi.org/10.1016/j.msec.2017.12.006
36. Liu DP, Zhang Y, Jiang GH et al (2018) Fabrication of dissolving microneedles with thermal-responsive coating for NIR-triggered transdermal delivery of metformin on diabetic rats. ACS Biomater Sci Eng 4(5):1687–1695. https://doi.org/10.1021/acsbiomaterials.8b00159
37. Jiang Q, Liu Y, Guo RR et al (2019) Erythrocyte-cancer hybrid membrane-camouflaged melanin nanoparticles for enhancing photothermal therapy efficacy in tumors. Biomaterials 192:292–308. https://doi.org/10.1016/j.biomaterials.2018.11.021
38. Van Den Bulcke AI, Bogdanov B, Rooze ND et al (2000) Structural and rheological properties of methacrylamide modified gelatin hydrogels. Biomacromol 1(1):31–38. https://doi.org/10.1021/bm990017d
39. Fonseca DFS, Costa PC, Almeida IF et al (2020) Swellable gelatin methacryloyl microneedles for extraction of interstitial skin fluid toward minimally invasive monitoring of urea. Macromol Biosci 20(10):2000195. https://doi.org/10.1002/mabi.202000195
40. Sun MY, Sun XT, Wang ZY et al (2018) Synthesis and properties of gelatin methacryloyl (GelMA) hydrogels and their recent applications in load-bearing tissue. Polymers 10(11):1290. https://doi.org/10.3390/polym10111290

41. Hoch E, Hirth T, Tovar GEM et al (2013) Chemical tailoring of gelatin to adjust its chemical and physical properties for functional bioprinting. J Mater Chem B 1(41):5675–5685. https://doi.org/10.1039/c3tb20745e
42. Li W, Terry RN, Tang J et al (2019) Rapidly separable microneedle patch for the sustained release of a contraceptive. Nat Biomed Eng 3(3):220–229. https://doi.org/10.1038/s41551-018-0337-4
43. Yu WJ, Jiang GH, Zhang Y et al (2017) Polymer microneedles fabricated from alginate and hyaluronate for transdermal delivery of insulin. Mater Sci Eng C 80(1):187–196. https://doi.org/10.1016/j.msec.2017.05.143
44. Sulllivan SP, Koutsonanos DG, Martin MD et al (2010) Dissolving polymer microneedle patches for influenza vaccination. Nat Med 16(8):915–920. https://doi.org/10.1038/nm.2182
45. Park JH, Allen MG, Prausnitz MR (2005) Biodegradable polymer microneedles: Fabrication, mechanics and transdermal drug delivery. J Contr Release 104(1):51–66. https://doi.org/10.1016/j.jconrel.2005.02.002
46. Fu Y, Kao WJ (2010) Drug release kinetics and transport mechanisms of non-degradable and degradable polymeric delivery systems. Expert Opin Drug Del 7(4):429–444. https://doi.org/10.1517/17425241003602259
47. Kim MY, Jung BY, Park JH (2012) Hydrogel swelling as a trigger to release biodegradable polymer microneedles in skin. Biomaterials 33(2):668–678. https://doi.org/10.1016/j.biomaterials.2011.09.074
48. Liu DP, Yu B, Jiang GH et al (2018) Fabrication of composite microneedles integrated with insulin-loaded $CaCO_3$ microparticles and PVP for transdermal delivery in diabetic rats. Mater Sci Eng C 90(1):180–188. https://doi.org/10.1016/j.msec.2018.04.055
49. Chang H, Zheng MJ, Yu XJ et al (2017) A swellable microneedle patch to rapidly extract skin interstitial fluid for timely metabolic analysis. Adv Mater 29(37):02243. https://doi.org/10.1002/adma.201702243
50. Yu WJ, Jiang GH, Zhang Y et al (2017) Near-infrared light-responsive and separable microneedles for transdermal drug delivery of metformin on diabetic rats. J Mater Chem B 5(48):9507–9513. https://doi.org/10.1039/C7TB02236K
51. Zhou G, Myers R, Li Y et al (2001) Role of AMP-activated protein kinase in mechanism of metformin action. J Clin Invest 108(8):1167–1174. https://doi.org/10.1172/JCI13505
52. Yang Z, Chai DN, Gao MY et al (2019) Thermal ablation of separable microneedles for transdermal delivery of metformin on diabetic rats. Int J Polym Mater Polym Biomater 68(14):850–858. https://doi.org/10.1080/00914037.2018.1517347
53. Chen BZ, Zhang LQ, Xia YY et al (2020) A basal-bolus insulin regimen integrated microneedle patch for intraday postprandial glucose control. Sci Adv 6(28):eaba7260. https://doi.org/10.1126/sciadv.aba7260
54. Yu JC, Wang JQ, Zhang YQ et al (2020) Glucose-responsive insulin patch for the regulation of blood glucose in mice and minipigs. Nat Biomed Eng 4(5):499–506. https://doi.org/10.1038/s41551-019-0508-y
55. Wu CY, Wang SG, Zhao JL et al (2019) Biodegradable Fe (III)@WS_2-PVP nanocapsules for redox reaction and time-enhanced nanocatalytic, photothermal, and chemotherapy. Adv Funct Mater 29(26):1901722. https://doi.org/10.1002/adfm.201901722